



## Flocs of fly ash-silicon-ferric coagulant based on the fractal dimension and research on flocculation

Juan Tan, Yanzhen Yu\*, Yong Sun, Lei Cheng

*School of Civil Engineering and Architecture, University of Jinan, Jinan 250022, China  
Tel. +86 53189736600; Fax: +86 53189736600; email: [tanjung745@gmail.com](mailto:tanjung745@gmail.com)*

Received 23 November 2012; Accepted 8 September 2013

### ABSTRACT

Fly ash-silicon-ferric coagulant prepared with fly ash extract and  $K_2FeO_4$  by co-polymerization is a new kind of inorganic polymer coagulant for lead wastewater treatment. Basicity and pH value, as important parameters, played a vital role in the preparation and polymerization of fly ash-silicon-ferric coagulant. In this experiment, fly ash-silicon-ferric coagulants were prepared with different basicities, pH values and molar ratios of  $Si/FeO_4^{2-}$ . The objective of this work is to study the influence of basicity, pH and molar ratio of  $Si/FeO_4^{2-}$  on physico-chemical properties and surface morphology of fly ash-silicon-ferric coagulant, and to research the influence of dosage and pH in raw water on the coagulation performance as well. To do so, scanning electron microscope and X-ray diffraction analyses were used to investigate the surface properties and morphology of flocs in coagulation based on the fractal dimension. Transmission electron microscope and infra-red spectroscopy were used to characterize the structure of fly ash-silicon-ferric coagulants. Results showed that the coagulant possessed branches shape structure. The comparison of coagulation efficiencies for turbidity, color, and  $Pb^{2+}$  was investigated by batch experiments. The results showed that the removal efficiencies of turbidity, color, and  $Pb^{2+}$  by fly ash-silicon-ferric coagulant were excellent in a lower dosage. The good coagulation efficiencies were 96% for  $Pb^{2+}$  removal, 98% for turbidity removal, and 90.5% for color removal.

*Keywords:* Fly ash-silicon-ferric; Coagulants; Flocs; Coagulation process

### 1. Introduction

Many types of complex coagulants are used in the wastewater treatment, such as poly aluminum chloride, polymeric phosphorus aluminum chloride, and so on. Their flocculation is better than that of a single aluminum salt coagulant [1–5]. But long-term experiments have proved that rudimental aluminum had latent toxicity which limited the development of

aluminum-based coagulants [6], so more researchers paid their attention to the iron-based coagulants [7–9]. Adding the iron salt, as the coupling of metal ions, to the poly-silicate, researchers obtain ploy-ferric-silicic coagulants, such as the PFSC and PFSS [10,11]. This kind of coagulant possess the function of electricity of ion salt and bridge network capture of activated silicic acid, at the same time it has well performance in removing turbidity and organics [12,13]. The PFSC is a kind of ferrosilicon coagulant developed in early 90s of the last century.

\*Corresponding author.

This study aims to investigate the use of fly ash extract for preparation of fly ash-silicon-ferric coagulant and treatment performance of lead wastewater. Using the transmission electron microscope (TEM) and infra-red (IR) analysis, the structure and spectra of coagulants prepared with different basicities and pH are analyzed to investigate the coagulation mechanism. After characterization of fly ash-silicon-ferric coagulants, the effects of dosage and pH on coagulation behavior are also studied by jar tests. Surface morphology and mineral identification of flocs in coagulation are characterized based on the fractal dimension. The results from the jar tests are compared to determine the best parameters.

## 2. Materials and methods

In this work, the reaction mode between Si and Fe qualitatively was studied using X-ray diffraction, ultra-violet/visible absorption (UVA) scanning, TEM, and IR, in which molar ratio of  $\text{Si}/\text{FeO}_4^{2-}$  and the reaction time was focused on. pH values were measured during the preparation of fly ash-silicon-ferric coagulant to reveal the relationship between characteristics and coagulation performance of the coagulant.

### 2.1. Preparation of fly ash-silicon-ferric coagulant

In this work, NaOH is analytical reagent diluted to 1.8 mol/L with deionized water before use. Then, it was introduced into fly ashes while stirring with magnetic stirring apparatus at 60°C. The fly ash extract was prepared after 10 h.  $\text{H}_2\text{SO}_4$  used for the preparation of fly ash-silicon-ferric coagulant was also analytical reagent and was diluted to 20% with deionized water. The silicic acid was prepared with 20%  $\text{H}_2\text{SO}_4$  and fly ash extract at room temperature (25°C).

In this respect, two approaches, copolymerization and composite algorithm, to the preparation of fly ash-silicon-ferric coagulant have been developed. The final pH value of the silicic acid prepared with 20%  $\text{H}_2\text{SO}_4$  and fly ash extract was adjusted about 1.4 to get good polymerization. PS solution was obtained after 1.5 h of polymerization.  $\text{K}_2\text{FeO}_4$  was dissolved in PS solution at  $\text{Si}/\text{FeO}_4^{2-}$  molar ratio of 3.5 at 45°C stirring with magnetic stirrer to obtain fly ash-silicon-ferric coagulant. Fly ash-silicon-ferric coagulant samples were taken out at different aging times, the coagulant samples dilution with different molar ratios of  $\text{Si}/\text{FeO}_4^{2-}$  (FASF2.0, FASF3.5, and FASF5.0 representing  $\text{Si}/\text{FeO}_4^{2-}$  2.0, 3.5, and 5.0, respectively) at

different reaction times were produced. The properties of coagulant were: density 1.50–1.56 g/cm<sup>3</sup>, pH 2.0–2.5, and turbidity 11.5–13.6 NTU.

### 2.2. Coagulation procedures

The raw water used in this study was made by lead nitrate (chemical grade) and surface water. The physico-chemical parameters of the raw water are summarized in Table 1.

To determine the influence of coagulation efficiency, experiments were carried out in 1.0 L Plexiglas beakers using a six paddle stirrer (JJ-4A agitator) according to the standard jar test. The coagulation procedure consisted of a rapid mix at 240 rpm for 1 min during coagulant addition, and 70 rpm for 8 min. Then, the flocs were allowed to settle for 15 min prior to water quality analysis.

### 2.3. Analytical methods

Turbidity were measured with a turbidimeter (HACH 2100Q, USA), pH was adjusted using an ORP instrument (HANNA, Italy). Color concentration was determined by a color analyzer (HI93727, HANNA, Italy). At the same time,  $\text{Pb}^{2+}$  measurements were performed by an atomic absorption (TAS-990AFG, China).

Liquid fly ash-silicon-ferric coagulant at the final reaction stage (as defined in the Results) was dried in an oven at 45°C (controlled exactly) for more than 12 h, then the powder samples were analyzed with D/max-rB X-ray diffractionmeter (Rigaku Corporation, Japan).

The solution of fly ash-silicon-ferric coagulant at different reaction times diluted by 400 times was scanned from 190 to 700 nm with UV-2552 spectrophotometer (Shimadzu, Japan).

The conductivity of fly ash-silicon-ferric coagulant was measured using DDS-11A digital conductivity with platinum black electrodes (Shanghai, China).

The species distribution and transformation of iron in fly ash-silicon-ferric coagulant was studied by means of Fe-Ferron complexation timed spectrophotometry.

TEM was carried out to identify the structure of the fly ash-silicon-ferric coagulant and to elucidate

Table 1  
Characteristics of raw water

|                          |     |
|--------------------------|-----|
| Temperature (°C)         | 25  |
| Turbidity (NTU)          | 260 |
| Color                    | 800 |
| $\text{Pb}^{2+}$ /(mg/L) | 20  |

whether basicity and pH had an effect on the structure and morphology of coagulants, using a transmission electron microscope (JEM-2010, Japan). Fly ash-silicon-ferric coagulants were also characterized by IR spectral analysis using an IR spectrometer (Nicolet 380, American). The spectra were taken from thin KBr pellets. The results of infra-red spectrometry of the physical structure and coagulation mechanics analysis are favorable. Prior to scanning electron microscope (SEM) analysis, flocs of coagulation were dried for further identification. The morphologies of flocs were obtained using a scanning electron microscope (S-2500, Hitachi, Japan). To obtain the relation between the fractal dimension and floc properties, flocs of coagulation were characterized using an X-ray diffractometer (D8 Advance, Bruker-AXS Company, Germany).

### 3. Results and discussion

#### 3.1. X-ray diffraction

Fig. 1 shows that the diffractive crystals spectra such as  $\text{Fe}_2\text{O}_3$ ,  $\text{Fe}(\text{OH})_3$ ,  $\text{Fe}_3\text{O}_4$ , and  $\text{SiO}_2$  could not be observed in FASF2.0 and FASF3.5, which indicated

that such materials as  $\text{Fe}^{3+}$  and PS were combined with the polymerization to form a new compound which was not included in the gallery. As can be seen from Fig. 1(c), more crystalline substances coexisted in FASF5.0 than in FASF2.0 and FASF3.5 suggesting that much more co-polymerized crystal-line of Al and Fe and many other ions were formed. Therefore, it could be suggested that some new kind of crystal compounds or some new crystal matters which do not give a standard formula maybe have been formed in fly ash-silicon-ferric coagulant. A possible reason for this was considered the higher molecular weight of fly ash-silicon-ferric coagulant molecules including three metals of Al, Fe, and the different characteristic groups, which induce hydrogen bonding, resulting in the formation of larger and amorphous chemical species during polymerization.

#### 3.2. UVA scanning spectra

Influence of reaction time and  $\text{Si}/\text{FeO}_4^{2-}$  ratios was studied. The UVA spectra of fly ash-silicon-ferric coagulant samples taken from different reaction time and  $\text{Si}/\text{FeO}_4^{2-}$  ratios are shown in Fig. 2.

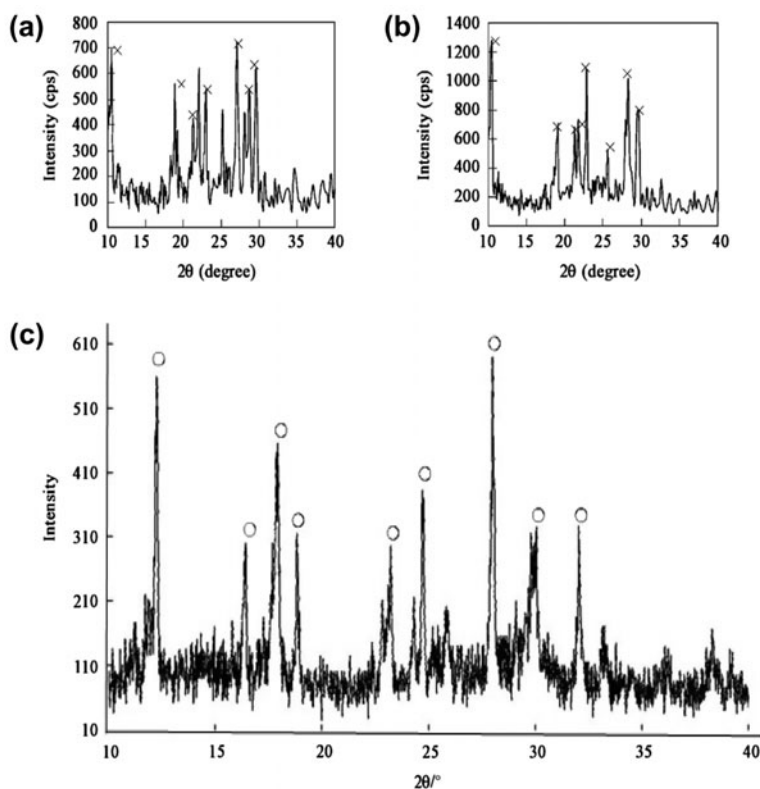


Fig. 1. X-ray diffractive analysis of crystal structure for fly ash-silicon-ferric coagulant with various  $\text{Si}/\text{FeO}_4^{2-}$  ratios: (a) FASF2.0; (b) FASF3.5; and (c) FASF5.0.

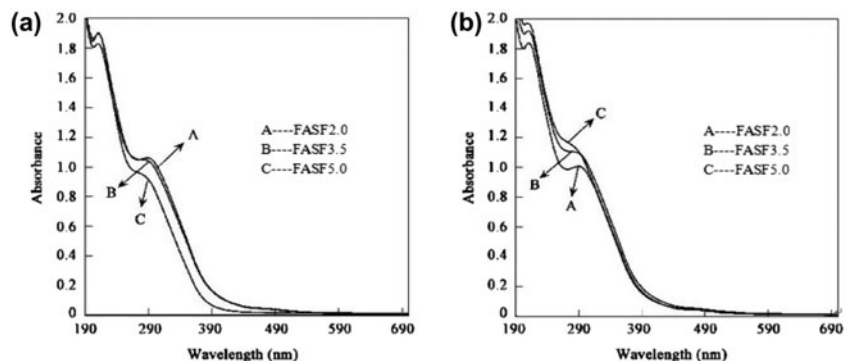


Fig. 2. Influence of  $\text{Si}/\text{FeO}_4^{2-}$  ratio on UVA spectra of fly ash-silicon-ferric coagulant at different reaction stages. (a) Initial reaction stage and (b) final reaction stage.

As revealed in Fig. 2, the characteristic peak at different reaction stages had an evident different change trend. At the initial stage, the absorbance decreased with increasing  $\text{Si}/\text{FeO}_4^{2-}$  ratio due to easy hydrolysis of  $\text{Fe}^{3+}$  at a higher  $\text{Si}/\text{FeO}_4^{2-}$  ratio, indicating that the amount of species which hydrolyzes easily increased with increasing the  $\text{Si}/\text{FeO}_4^{2-}$  ratio. At the final stage, the absorbance increased with increasing the  $\text{Si}/\text{FeO}_4^{2-}$  ratio due to the difficult hydrolysis of  $\text{Fe}^{3+}$  at a higher  $\text{Si}/\text{FeO}_4^{2-}$  ratio, which demonstrated that the amount of species which hydrolyzed easily decreased with increasing the  $\text{Si}/\text{FeO}_4^{2-}$  ratio. It was shown that the gelation rate of fly ash-silicon-ferric coagulant during the preparation increased with decreasing the  $\text{Si}/\text{FeO}_4^{2-}$  ratio in the experimental phenomena.

### 3.3. Conductivity of fly ash-silicon-ferric coagulant

Influence of aging time and  $\text{Si}/\text{FeO}_4^{2-}$  ratios on conductivity in the preparation process of fly ash-silicon-ferric coagulant is shown in Fig. 3. The conductivity was mainly analyzed according to the influence of  $\text{Si}/\text{FeO}_4^{2-}$  ratios on the aging time change.

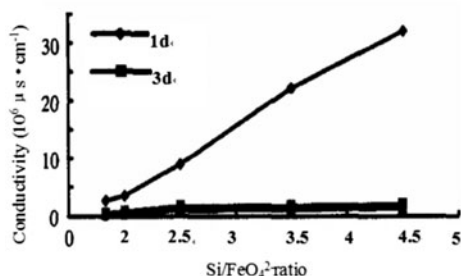


Fig. 3. Influence of  $\text{Si}/\text{FeO}_4^{2-}$  ratio on conductivity of fly ash-silicon-ferric coagulant at different aging times.

Fig. 3 displays the impact of aging time on conductivity change at different  $\text{Si}/\text{FeO}_4^{2-}$  ratios. The conductivity increased with increasing the  $\text{Si}/\text{FeO}_4^{2-}$  ratio when aging time was 1 day. It was indicated that  $\text{Fe}^{3+}$  hydrolyzed into high ions except the other reacting with PS. Furthermore, the conductivity decreased with increasing the aging time and rapid decline at the initial stage. The charge number was reduced in

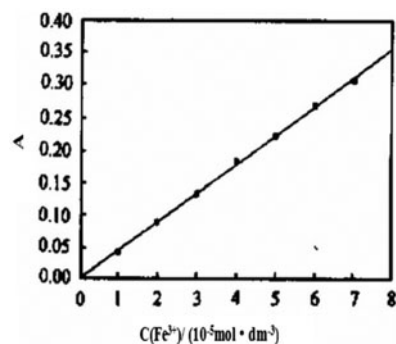


Fig. 4. Fe-Ferron timed complexation spectrophotometry standard curve.

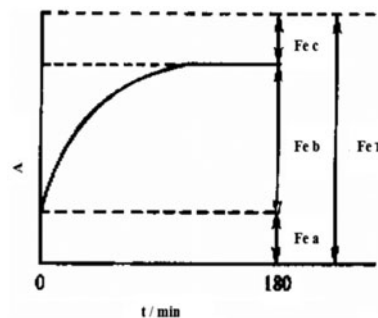


Fig. 5. Fe-Ferron timed complexation spectrophotometry work curve.

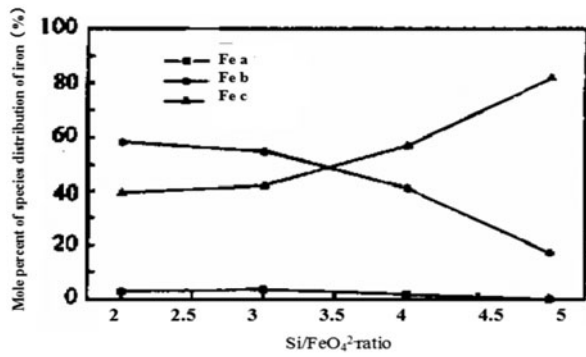


Fig. 6. The species distribution of iron in fly ash-silicon-ferric coagulant with different Si/FeO<sub>4</sub><sup>2-</sup> ratios.

the solution of fly ash-silicon-ferric coagulant at the initial stage of the aging time. At the final stage of the aging time, the conductivity decreased slowly because the reaction rate slowed down in the polymerization of Fe<sup>3+</sup> and PS.

### 3.4. Fe-Ferron complexation timed spectrophotometry

Fe-Ferron timed complexation spectrophotometry standard curve was drawn using the acid standard solution of iron (Fig. 4). Combined with the standard curve and the Fe-Ferron timed complexation spectrophotometry work curve (Fig. 5), can be quantitatively calculated the mole percents of Fe<sub>a</sub>, Fe<sub>b</sub>, and Fe<sub>c</sub> in the fly ash-silicon-ferric coagulant samples [14].

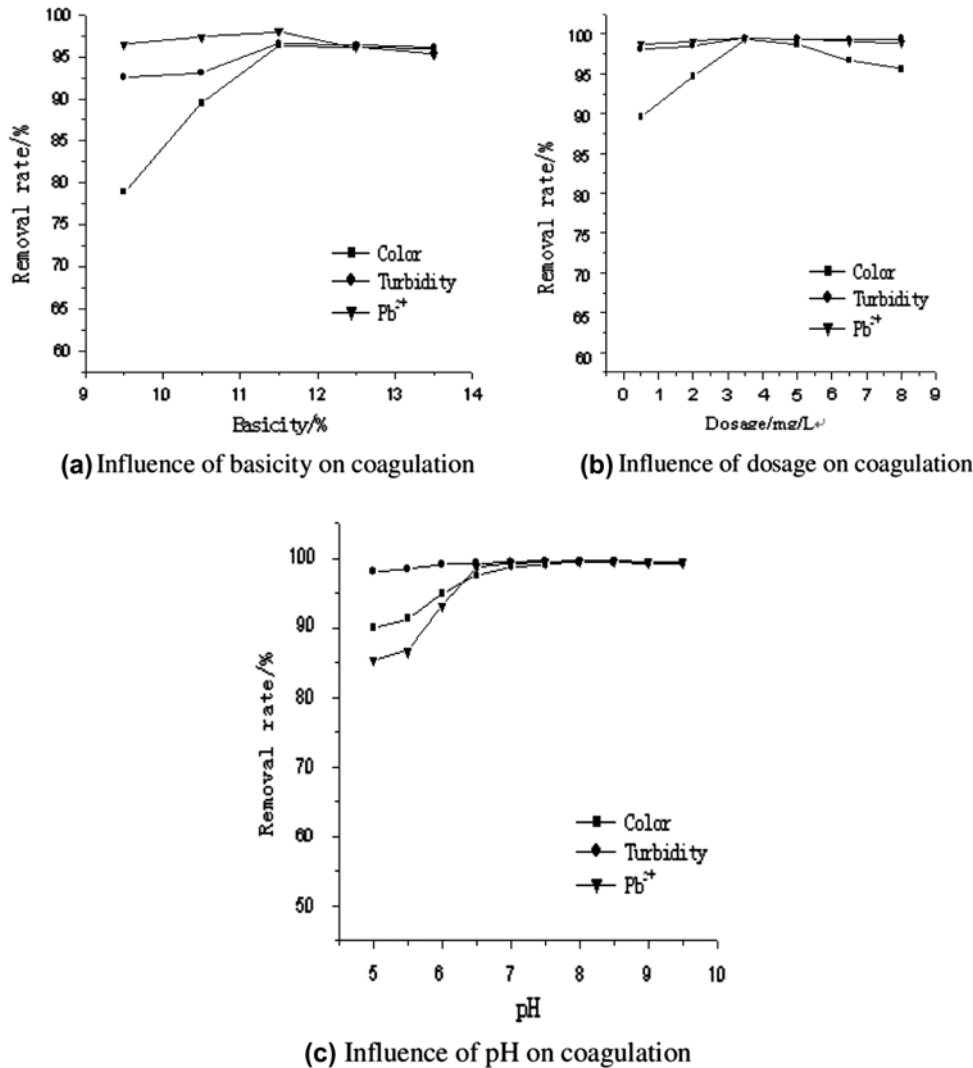


Fig. 7. Coagulation efficiency of different parameters on turbidity, color, and Pb<sup>2+</sup> removal.

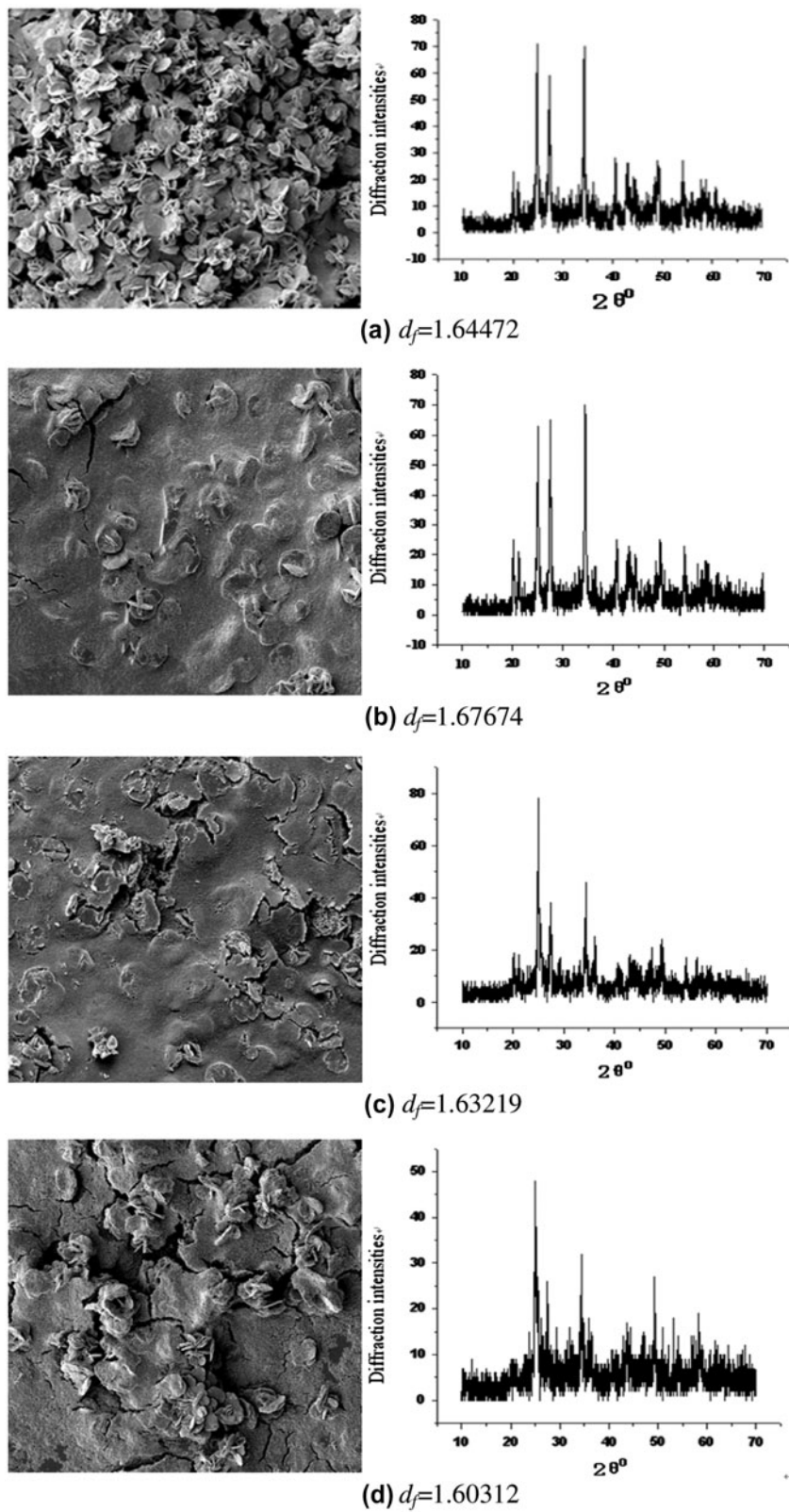


Fig. 8. The fractal SEM structure photos and XRD spectrum at different dosages ( $a = 2.10$  mg/L;  $b = 4.50$  mg/L;  $c = 6.00$  mg/L; and  $d = 8.07$  mg/L).

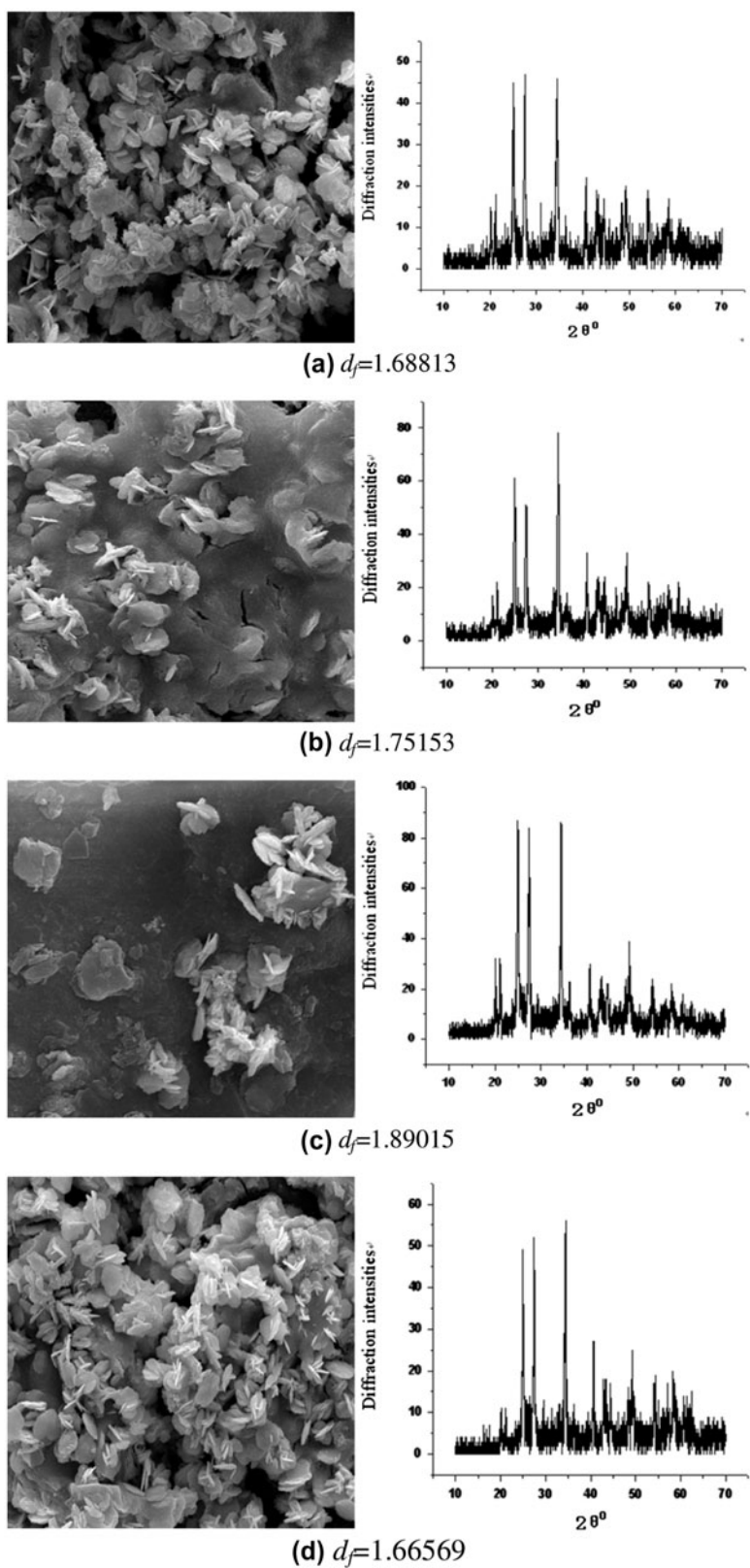


Fig. 9. The fractal SEM structure photos and XRD spectrum in different pH values (a) pH 7.5; (b) pH 8.5; (c) pH 9.5; and (d) pH 10.

According to the different hydrolysis of iron with ferron at different rates, the form of iron can be divided into three parts ( $Fe_a$ ,  $Fe_b$ , and  $Fe_c$ , respectively).  $Fe_a$  refers to the iron whose reaction with ferron is instantaneous.  $Fe_b$  refers to the polymer of iron in low degree of polymerization.  $Fe_c$  refers to the polymer of iron in high degree of polymerization.  $Fe_T$  refers to the sum total of various forms of iron.

As seen from Fig. 6, mole percent of  $Fe_a$  changed little with increasing the  $Si/FeO_4^{2-}$  ratio, its value decreased slowly. While mole percent of  $Fe_b$  decreased greatly, its range decreased faster with increasing the  $Si/FeO_4^{2-}$  ratio. Contrary to the change trend of  $Fe_b$ , the mole percent of  $Fe_c$  showed a rising trend. It suggests that the species of iron in fly ash-silicon-ferric coagulant change from  $Fe_a$  and  $Fe_b$  to  $Fe_c$ . The results showed that the species of iron changed from lower polymer to higher polymer with increasing the  $Si/FeO_4^{2-}$  ratio.

### 3.5. Performance of fly ash-silicon-ferric coagulant in lead water treatment

The influences of basicity, dosage, and pH on the coagulation procedures were investigated. As important parameters, basicity, dosage, and pH had a great effect on the flocculation efficiency of fly ash-silicon-

ferric coagulant. Fig. 7 illustrates the flocculation efficiency at different parameters.

Fig. 7 shows that color, turbidity, and  $Pb^{2+}$  removal rate tend to increase in varying degrees with the salt-basicity increase. The salt-basicity is the main influencing factor resulting in the morphological changes of iron hydrolysis. Salt-basicity had greater influence on the color removal rate. The removal rate of turbidity and  $Pb^{2+}$  was higher than 90% at different salt-basicities. Thus, salt-basicity of the fly ash-silicon-ferric coagulant affects mainly the removal of color, and it has an important influence on the stability of coagulant.

The removal rate of color had a significant upward trend with the increase of the coagulant dosage. But color removal rate was stabilized when the dosage was about to 4.5 mg/L. When the dosage of coagulant continued to increase, the color removal rate was on a downward trend. The removal efficiency of turbidity and  $Pb^{2+}$  was more than 95%, and removal rates were very stable under different coagulant dosages. It was clear that fly ash-silicon-ferric coagulant had a superior coagulation in lead water treatment under a low dosage.

Color, turbidity, and  $Pb^{2+}$  removal rates all tended to increase in varying degrees with the increase of pH in raw water. The extent of increasing removal of  $Pb^{2+}$

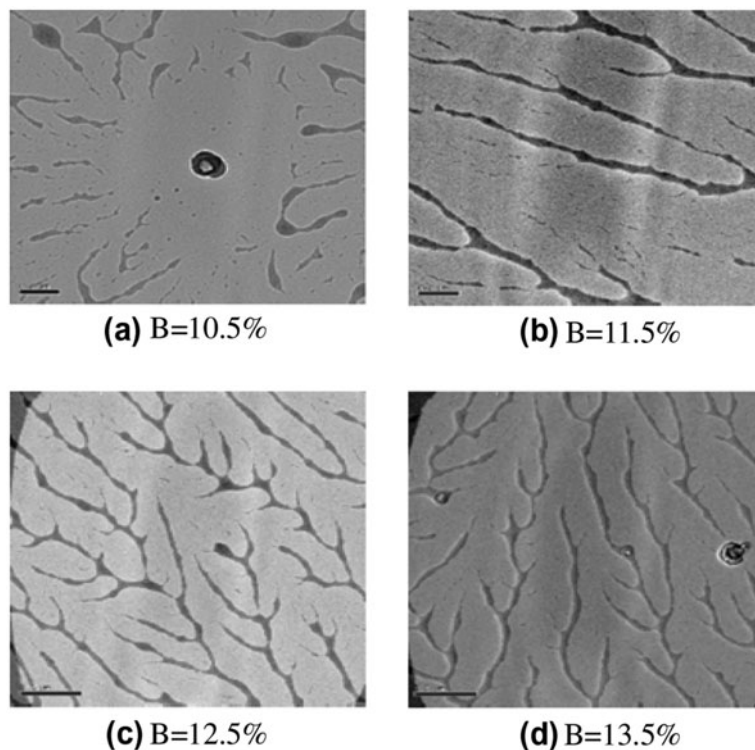


Fig. 10. Impact of basicity on the microstructure of coagulant.



was the largest. As an important parameter, pH had a great effect on  $\text{Pb}^{2+}$  removal. Therefore, fly ash-silicon-ferric coagulant could effectively remove  $\text{Pb}^{2+}$  from raw water at suitable pH.

### 3.6. Relationship between the fractal dimension and flocs surface microstructure

There was a direct relevancy between flocs of fly ash-silicon-ferric coagulant and  $\text{Pb}^{2+}$  removal. Owing to the different coagulant dosages with different pHs, the removal rates of  $\text{Pb}^{2+}$  differed greatly. The SEM (4,000 $\times$ ) and IR analysis of flocs which were obtained at different coagulant dosages are shown in Fig. 8, and the SEM (4,000 $\times$ ) and IR analysis of flocs which were obtained as different pHs in raw water are shown in Fig. 9.

XRD patterns (Fig. 8) show that there were many compounds containing Si, Fe, and Pb in the flocs. As shown in Fig. 8, the first two wave peaks of XRD pattern were lower when the coagulant dosage was

2.10 mg/L. Numerous small clusters of floc surface morphology are shown in the SEM photograph. It can be seen that floc surface structure loosened and the fractal dimension was smaller when the  $\text{Pb}^{2+}$  removal rate was low. The clusters of floc would reduce and floc surface structure became dense with the increase of the dosage. The fractal dimensions reached maximum when the dosage was 4.5 mg/L. But, there was a reverse trend for floc surface structure when the dosage increased continuously, and the  $\text{Pb}^{2+}$  removal rate was lower.

SEM photographs (Fig. 9) show that the floc surface morphology at different pHs was different under the same coagulant dosage. The pH value had an obvious influence on the surface morphology and the structure of flocs. In terms of fly ash-silicon-ferric coagulant, higher pH was favorable to the hydrolysis of poly ferric, and then aggregation clusters were formed. The floc surface structure became dense and the fractal dimension increased with the increase of pH in raw water from 7.5 to 9.5. Compared with

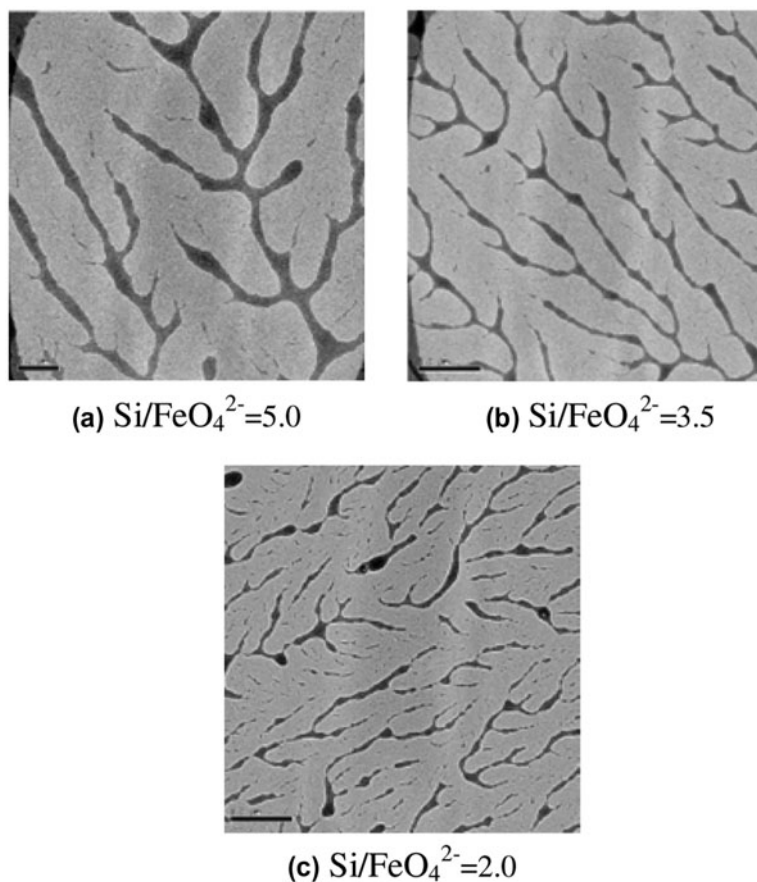


Fig. 11. Impact of  $\text{Si}/\text{FeO}_4^{2-}$  on the microstructure of coagulant.

different pH values, better cluster of floc structure was formed which contributed to good coagulation performance.

In order to assure the relationship between the fractal dimension and flocs SEM structure, the test was conducted with the flocs. SEM photographs, and XRD measuring after flocs drying revealed that the flocs structure was most regular and meticulous; the fractal dimension was the biggest at optimum coagulation conditions. Analyzing the relationship between the fractal dimension of flocs and the lead removal, a good correlation between them can be seen. The degree of coagulation and the treatment effect was reflected by measuring the fractal dimension and SEM structure.

### 3.7. Effect of basicity and $\text{Si/FeO}_4^{2-}$ on microstructure of fly ash-silicon-ferric coagulant

The basicity and  $\text{Si/FeO}_4^{2-}$  of coagulant was measured by TEM (magnifies 10,000 diameters) to

determine the ability for the microstructure of coagulant as presented in Figs. 10 and 11.

TEM photographs (Fig. 10) show that the sample did not form an obvious crystal and branching structure, and the branch chain was short and discontinuous at low salt-basicity. With the salt-basicity increase, the sample gradually revealed a branched structure. When the salt-basicity was 11.5%, the coagulant sample had a continuous branched structure, but the structure was rare. The figure shows that salt-basicity relates to the branched structure of the coagulant.

As shown in Fig. 11, the branching shape of the coagulant structures had a certain disparity at different  $\text{Si/FeO}_4^{2-}$  ratios. When the  $\text{Si/FeO}_4^{2-}$  was 2.0, there was some branch-shaped structure, but the branched structure was not obvious. With the increase of  $\text{Si/FeO}_4^{2-}$ , the group of branches became more clear and the diameter tended to reduce. It could be seen from Fig. 11 that the morphology and structure of the coagulants were different at different  $\text{Si/FeO}_4^{2-}$  ratios. Furthermore, with the continuous

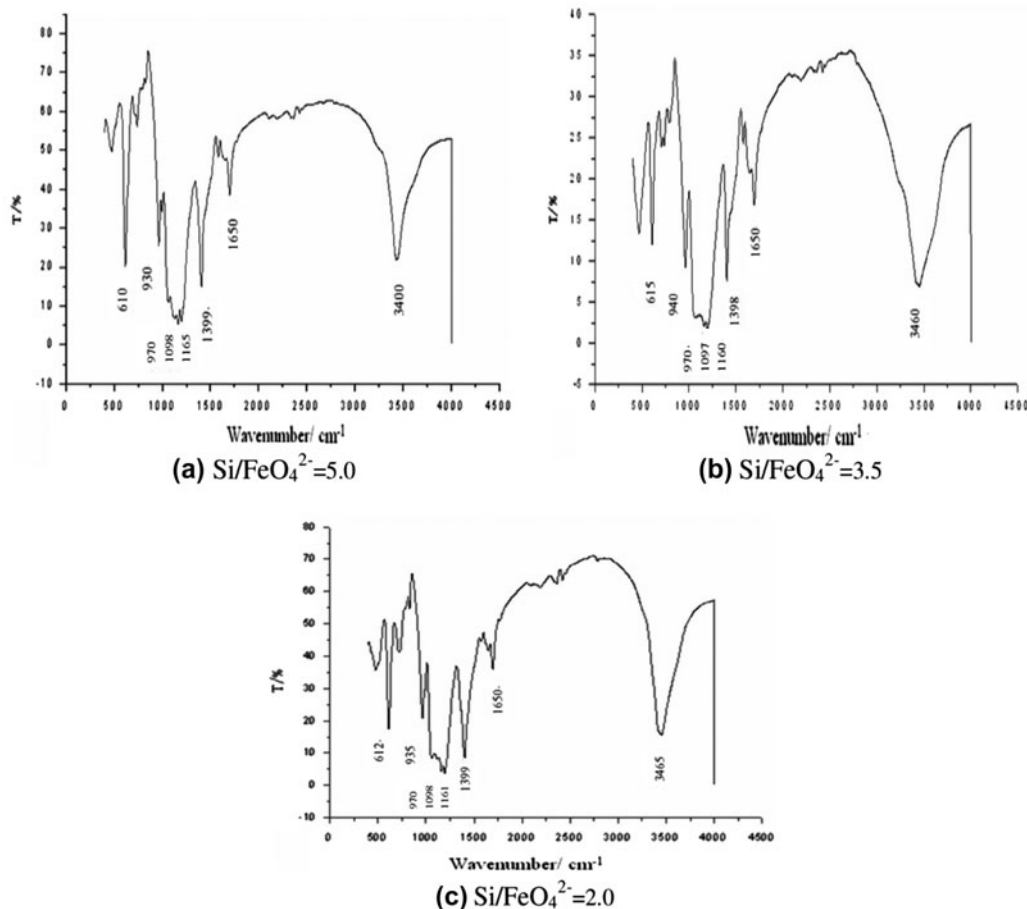


Fig. 12. Infrared spectrum of coagulant with different  $\text{Si/FeO}_4^{2-}$ .

increase of the  $\text{Si}/\text{FeO}_4^{2-}$  ratio, many short and small branches appeared. The results show that a higher polymer was formed in the polymerizing process.

### 3.8. Effect of $\text{Si}/\text{FeO}_4^{2-}$ on IR structure of fly ash-silicon-ferric coagulant

IR spectrometry plays an important role in the research of polymer for chemical property, stereo structure, sequential state, and so on. The infra-red absorption spectra of fly ash-silicon-ferric coagulants with different  $\text{Si}/\text{FeO}_4^{2-}$  were recorded (Fig. 12).

As shown in Fig. 12, fly ash-silicon-ferric coagulants with different  $\text{Si}/\text{FeO}_4^{2-}$  were somewhat similar. The spectrum showed that the  $\text{OH}^-$  groups stretching vibration absorption peak was at  $3,650\text{--}3,200\text{ cm}^{-1}$ , so it could make sure the presence of the  $\text{OH}^-$  groups. The peak around  $940\text{ cm}^{-1}$  was attributed to the Si–O–Al or Si–O–Fe bands [15,16].  $1,650\text{ cm}^{-1}$  expressed the bending vibration absorption peak of the absorbed water, coordinated water, and crystal water. There were absorption peaks at around  $1,099\text{ cm}^{-1}$  wave number attributed to the asymmetric stretching vibration of Fe–OH–Fe or Al–OH–Al [15,16]. The peak around  $1,162\text{ cm}^{-1}$  was the Si–O groups stretching vibration absorption peak. And the band located at  $1,399\text{ cm}^{-1}$  was attributed to the goethite FeOOH. The peak around  $970\text{ cm}^{-1}$  denoted the Si–O–Fe band. It indicated that the coagulant was complex according on the Si–O–Fe–O–Fe–O–Si band. Nearby  $470\text{--}620\text{ cm}^{-1}$ , was the main Fe–O groups stretching vibration absorption peak. With the decrease of the  $\text{Si}/\text{FeO}_4^{2-}$  molar ratio, the order of the Si–O–Fe absorption peak intensity was  $3.5 > 2 > 5$ .

## 4. Conclusions

This investigation showed flocs of fly ash-silicon-ferric coagulants with different dosage and pH, different characterization on surface structure, micro-structure, coagulation performance.

It showed that the factors affecting the removal of color, turbidity, and  $\text{Pb}^{2+}$  effects are hydrolysis products of iron in the fly ash-silicon-ferric coagulant. The removal of color, turbidity, and  $\text{Pb}^{2+}$  is influenced mainly by the hydroxyl complex.

There was an obvious difference in the surface morphology and the absorption peak of flocs prepared with different coagulant dosages and pH in raw water by SEM image and XRD analysis.

Compounding the fly ash extract and potassium ferrate, the hydrolyzate products were influenced by the salt-basicity and  $\text{Si}/\text{FeO}_4^{2-}$  ratio. The coagulant

morphology was observed by using the transmission electron microscopy; it could get some more intuitive information. The results showed that different salt-basicities and  $\text{Si}/\text{FeO}_4^{2-}$  ratios could have some impact on the coagulant morphology. The increase of the salt-basicity helped to improve the degree of polymerization and promoted the branch chain structure formation. The  $\text{Si}/\text{FeO}_4^{2-}$  ratio was the determining factor for the density of branch chain structure and the size of the twig diameter.

Fly ash-silicon-ferric coagulant is found to be essentially a complex compound of Si, Al, Fe, and other ions, instead of a simple mixture of raw materials. The qualitative investigation of the reaction mode between Si and Fe in fly ash-silicon-ferric coagulant provides a certain theoretical basis for developing more effective and stable coagulants. In addition, much clearer understanding about the effect of  $\text{Si}/\text{FeO}_4^{2-}$  ratio on the species transformation has been obtained.

## Acknowledgment

This work was funded by the National Scientific Foundation China (No. 51178207), Shandong Provincial National Science Foundation (No. ZR2011EEM003), the Education Department of Shandong province university science, and technology project (No. J12LG52).

## References

- [1] C. Volk, K. Bell, E. Ibrahim, D. Verges, G. Amy, M. LeChevallier, Impact of enhanced and optimized coagulation on removal of organic matter and its biodegradable fraction in drinking water, *Wat. Res.* 34 (2000) 3247–3257.
- [2] M. Fan, R.C. Brown, T.D. Wheelock, A.T. Cooper, M. Nomura, Y. Zhuang, Production of a complex coagulant from fly ash, *Chem. Eng. J.* 106 (2005) 269–277.
- [3] M. Miyake, Y. Kimura, T. Ohashi, M. Matsuda, Preparation of activated carbon-zeolite composite materials from coal fly ash, *Micropor. Mesopor. Mater.* 112 (2008) 170–177.
- [4] A.M. Tenny, J. Derka, Hydroxylated ferric sulphate—An aluminium salt alternative, *Water Suppl. Manage.* 10(4) (1992) 167–174.
- [5] H.X. Tang, Z.K. Luan, Features and mechanism for coagulation–flocculation processes of polyaluminum chloride, *J. Environ. Sci.* 7(2) (1995) 204–211.
- [6] S.J. Santosa, E.S. Kunarti, J. Karmanto, Synthesis and utilization of Mg/Al hydrotalcite for removing dissolved humic acid, *Appl. Surf. Sci.* 254 (2008) 7612–7617.
- [7] W.P. Cheng, Comparison of hydrolysis/coagulation behaviour of polymeric and monomeric iron coagulants in humic acid solution, *Chemosphere* 47 (2002) 963–969.

- [8] A.I. Zouboulis, P.A. Moussas, F. Vasilakou, Poly ferric sulphate: Preparation, characterization and application in coagulation experiments, *J. Hazard. Mater.* 155(3) (2008) 459–468.
- [9] M. Fan, S. Sung, R.C. Brown, T.D. Wheelock, F.C. Laabs, Synthesis, characterization and coagulation of polymeric ferric sulphate, *J. Environ. Eng.* 128(6) (2002) 483–490.
- [10] J.K. Edzwald, J.E. Tobiason, Enhanced coagulation: US requirement and a broader view, *Water Sci. Technol.* 40(9) (1999) 63–70.
- [11] F. Julien, B. Güeroux, M. Mazet, Comparison of organic compound removal by coagulation-flocculation and by adsorption onto preformed hydroxide flocs, *Water Res.* 28 (1994) 2567–2574.
- [12] S. Stoll, J. Buffle, Computer simulation of bridging flocculation processes: The roles of chain conformation and chain/colloid concentration ratio in the aggregation structure, *J. Colloid Interf. Sci.* 205 (1998) 290–304.
- [13] S. Biggs, M. Habgood, G.J. Jameson, Y.-d. Yan, Aggregate structures formed via a bridging flocculation mechanism, *Chem. Eng. J.* 80 (2000) 13–22.
- [14] B. Tian, H. Tang, Determination of polymeric Fe(III) species by ferron-complexation timed spectrophotometric method, *Environ. Chem.* 8(4) (1989) 27–31.
- [15] T. Sun, C.-h. Sun, G.-l. Zhu, X.-j. Miao, C.-c. Wu, S.-b. Lv, W.-j. Li, Preparation and coagulation performance of poly-ferric-aluminum-silicate-sulfate from fly ash, *Desalination* 268 (2011) 270–275.
- [16] Y. Fu, S.L. Yu, Y.Z. Yu, L.P. Qiu, B. Hui, Reaction mode between Si and Fe and evaluation of optimal species in poly-silicic-ferric coagulant, *J. Environ. Sci.* 19 (2007) 678–688.